Asteroid 21 Lutetia at 3 μm: Observations with IRTF SpeX

Andrew S. Rivkin[1*], Beth E. Clark[2*], Maureen Ockert-Bell[2], Eric Volquardsen[3*], Ellen S. Howell[4], Schelte J. Bus[3], Cristina A. Thomas[5*], Michael Shepard[6]

1. **Johns Hopkins University Applied Physics Laboratory, 11100 Johns Hopkins Rd., Laurel MD 20723**
2. **Physics Department, Ithaca College, 953 Danby Road, Ithaca NY 14850**
3. **Institute for Astronomy, 640 N. Aohoku Place, Hilo HI 96720**
4. **Arecibo Observatory, HC 3 Box 53995, Arecibo PR 00612**
5. **Northern Arizona University, PO Box 6010, Flagstaff AZ 86011**
6. **Dept. of Geography and Geoscience, Bloomsberg University, 400 E. Second St., Bloomsburg PA 17815**

Submitted to Icarus
4 April 2011

Revised 10 August 2011

*The IRTF is operated by the University of Hawaii under Cooperative Agreement no. NCC 5-538 with the National Aeronautics and Space Administration, Office of Space Science, Planetary Astronomy Program.

Abstract:

We present observations of asteroid 21 Lutetia collected 2003-2008 using the SpeX instrument on the NASA Infrared Telescope Facility (IRTF) covering 2-4 μm. We also reevaluate NSFCam observations obtained in 1996 (Rivkin et al. 2000). Taken together, these show deeper 3-μm band depths (of order 3-5%) in the southern hemisphere of Lutetia, and shallower band depths (of order 2% or less) in the north. Such variation is consistent with observations at shorter wavelength by previous workers (Nedelcu et al. 2007, Lazzarin et al. 2010), who observed hemispheric-level variations from C-like spectra to X-like spectra.

While the shallowness of absorption bands on Lutetia hinders identification of its surface composition, goethite appears plausible as a constituent in its southern hemisphere (Beck et al. 2010). Mathematical models of space weathered goethite are most consistent with Lutetia's southern hemisphere spectrum, but more work and further observations are necessary to confirm this suggestion.

1. Introduction and Motivation

In 2004, the asteroids 21 Lutetia and 2867 Šteins were selected for an encounter with the European Space Agency's Rosetta spacecraft. Barucci et al. (2005) reviews what was known of Lutetia, Šteins, and the other candidate objects and the reasoning for choosing these objects. Earth-based observations of Lutetia have returned a confusing picture of the asteroid. It was assigned to the M class by Tholen (1984) based on its Eight Color Asteroid Survey (ECAS) spectrum. This class was largely associated with metallic objects at the time, and Lutetia was thus expected to have a metallic surface or perhaps an enstatite chondrite composition (Gaffey et al. 1989). Expanded spectral coverage (to 2.5 μm) by the 52-color survey led Howell et al. (1994) to perform a neural-net based classification. Lutetia showed some affinity to the C asteroids in this dataset (specifically the Cv subgroup, which includes 13 Egeria among others), but its high IRAS albedo (0.221, Tedesco et al. 1992) led Howell et al. to reject the Cv assignment and classify it only as M. Spitzer Space Telescope observations by Barucci et al. (2008) found Lutetia's 5-38 μm spectra to be most consistent with CO3 and CV3 carbonaceous chondrite meteorites. Observations by Bus and Binzel (2002a) led to an Xk classification in the Bus system, and increasing the long-wavelength end of the higher-resolution data to 2.5 μm results in a Xc classification in the Bus-DeMeo system (DeMeo et al. 2009). Rivkin et al. (2000) included Lutetia in their W class, defined as M asteroids with 3-μm absorptions (see below). Further discussion of these classifications in light of possible variation on Lutetia's surface is presented in Section 4.1.

Rivkin et al. (2000) presented spectrophotometric observations of Lutetia in the 1.5-3.5 μm region, finding it to have a band depth of 6.2 +/- 4.3% at 2.95 μm relative to an extrapolated continuum. This was interpreted as evidence for hydrated minerals and against an iron meteorite-like composition. Birlan et al. (2006) found only a shallow absorption in the 3 μm region, and no band near 3.1 μm. They suggested Lutetia's spectrum was at least qualitatively similar to that of the CV/CO meteorites.

Non-spectral information also has pointed away from a metallic composition for Lutetia: experiments by Magri et al. (1999) found a radar albedo consistent with C and S asteroids and lower than expected for high-metal objects like 216 Kleopatra. Shepard et al. (2008), using radar CW and delay-Doppler imaging observations confirmed the reported radar albedo and placed significant constraints on Lutetia's size. Both sets of observations (Oct, 1985 and Oct 2004) had sub-radar latitudes within a few degrees of Lutetia's south pole. Using an empirical radar model, Shepard et al. (2010) suggested that Lutetia's regolith contains more metal than ordinary or carbonaceous chondrites and suggested enstatite chondrites (EH) or exotic carbonaceous chondrites (e.g. CH/CB) as better analogs. Lupishko and Belskaya (1989) concluded that Lutetia (and other M asteroids) had a surface that is "not purely metallic" with "considerable silicate components". The albedo of Lutetia has been surprisingly difficult to pin down. Lamy et al. (2010) reviewed the situation, arguing that its geometric albedo is either 0.13 or 0.18, depending on the assumed phase function, and that discrepancies in the literature can be reconciled with one another if one accounts for the differing phase functions.

Rosetta encountered Lutetia in July 2010, with a flyby distance of roughly 3100 km. In anticipation of the release of those data and their interpretation, we collect hitherto unpublished observations of Lutetia in the 2-4 μm spectral region and reconsider the interpretation of Rivkin et al. (2000) in light of those observations.

2. Observations and Data Reduction:

Lutetia was observed on three separate occasions using the SpeX instrument in LXD (long-wavelength cross-dispersed) mode on the NASA Infrared Telescope Facility (IRTF), in 2003, 2007, and 2008. LXD mode covers the 1.9-4.2 μm spectral region with five overlapping orders, here we concentrate only on the 2.2-4.0 μm portion, omitting the shortest-wavelength order. The overlaps occur in the 2.54-2.73 μm, 2.96-3.12 μm, and 3.55-3.64 μm regions, and fine structure observed in those wavelength ranges is usually due to imperfect calibration at the edges of these orders.

Table 1 shows the observational circumstances including standard stars used on each night and the total integration time on Lutetia. Each exposure was 15 seconds, though the number of co-adds before a beam switch varied from 1-4.

Data reduction was conducted with the Spextool package of IDL routines, provided by the IRTF (Cushing et al. 2003). After the spectral extraction, a second set of IDL routines was used to fit and remove the signature of the Earth's atmosphere. This procedure has been used in several published works in both the 1-2.5 μm and 2-4 μm regions (Volquardsen et al. 2007, Binzel et al. 2009, Rivkin and

Emery 2010). One of the parameters of the atmospheric model is the best-fit value of the precipitable water (PW). The average values during each observation (0.97 ± 0.03 and 2.74 ± 0.15 in 2007 and 2008 respectively) are good matches to the values of PW calculated using the 225 GHz observations accumulated by the Caltech Submillimeter Observatory (CSO)[1] over the course of those same nights (0.97 ± 0.13 and 2.39 ± 0.31 for the times bracketing the LXD observations). Unfortunately, 225 GHz observations are not available for PW comparison for 2 March 2003. As with the order overlap mentioned above, imperfect atmospheric correction can cause apparent high-frequency spectral structure.

The temperatures of main belt asteroids are sufficiently high that the longest wavelengths considered here (beyond roughly 3.5 μm) are mixtures of both reflected sunlight and thermal emission from the asteroids themselves. In order to analyze the reflectance-only spectrum, thermal models have been developed and used to fit and remove the thermal emission, which in some cases also allows a study of the thermal properties (for instance, Rivkin et al. 2006). Increasingly sophisticated models have been developed for rapid rotators, unusual shapes, high themal inertias, etc. However, most large main belt asteroids like Lutetia are well fit by simpler models like the Standard Thermal Model (STM, Lebofsky et al. 1986) which we use here, modified by not fixing the beaming parameter at 0.756 (see below). The inputs to the STM are well-constrained for Lutetia, including most physical properties and ephemeris quantities (such as phase angle, solar, and Earth

[1] Overview of the JCMT By H.E. Matthews, J. Leech; 10 November 2004
http://docs.jach.hawaii.edu/JCMT/OVERVIEW/tel_overview/

distances), leaving only a single parameter to be fit, the beaming parameter (η). The STM assumes a spherical, non-rotating object (or equivalently, an object with no thermal inertia). The beaming parameter incorporates the effects of shape, rotation rate, and thermal inertia and allows modeling the object's temperature to fit the data without explicitly modeling surfaces or shapes. In general, objects with higher thermal inertia have $\eta > 1$, while $\eta < 1$ is commonly seen among large main belt asteroids (Delbó et al. 2007). Values of η less than 1 mean that the temperature is higher than what one might expect, often ascribed to surface roughness at the wavelength scale, attributable to craters and surface features that preferentially "beam" flux toward the observer compared to a perfectly smooth surface. We assume an emissivity of 0.9 for these thermal models, as is commonly done, and reasonable for most rocks.

The SpeX data analyzed here all are fit with $\eta \sim 0.75$-0.8 using a geometric albedo of 0.22 (Tedesco et al. 1992). This is comparable to the smallest beaming parameters seen among the main belt asteroids (Delbó et al. 2007). Using a lower albedo (0.13) as suggested by some workers results in a relatively small change in η to $\sim$0.9, still within the range commonly seen among large main belt asteroids. Reanalysis of the 1996 NSFCam photometric data suggests those data are most consistent with $\eta \sim 0.9$ (using the IRAS albedo of 0.22). These values for the beaming parameter are indirect evidence for a low thermal inertia regolith covering Lutetia's surface. The sub-solar point temperatures indicated for Lutetia with these parameters are in the 260-270 K range, varying with distance from the Sun. It is not clear why η differs between the spectrophotometric and spectroscopic

observations. While η is known to vary with phase angle (Delbo et al. 2003) the values of η we see are not correlated with the phase angle of the observations.

3. Results:

Figure 1 shows the spectra of Lutetia for each of the three SpeX observing runs. These have been normalized to 2.3 μm and offset from one another for clarity. In each case the spectrum shortward of 2.5 μm is quite flat, and the data longward of the atmospheric water gap is usually below the level of the continuum at shorter wavelengths. The band depths are rather modest in the SpeX data, only on the order of 1-2% at ~3.1-3.2 μm in 2003 and 2007, and roughly 5% in 2008 at those same wavelengths, as measured by reflectance below the values measured at 2.2-2.4 μm. The shallow bands in the 2003/2007 data are also punctuated by smaller-scale structure, though we believe this is due to incomplete removal of order overlap. The smoother 2008 spectrum is a better representation of the band shape. Appending additional datasets (Section 4.1) and extrapolating a continuum from the 2.0-2.5 μm region through the 3-μm region results in qualitatively similar but slightly smaller band depths (~3-5% in 2008 and ~0-1% in 2003/2007). As mentioned above, Rivkin et al. (2000) reported a band depth of ~6 +/- 4% at 2.95 μm, consistent with the 2008 observation and consistent with the 2003 and 2007 observations at the 1.5-σ level. These band depths used a continuum extrapolated from 1.65-2.4 μm.

3.1 Revisiting the 1996 measurements:

The availability of newer spectroscopic data and their difference from the spectrophotometric data led us to reconsider the 1996 observations and whether the discrepancies reflect real variation on Lutetia's surface or a miscalibration of the older data. We therefore considered the data obtained on each night individually rather than the published averages. In addition, we compared NSFCam and SpeX measurements of other objects observed on the same nights as Lutetia, in order to qualify the repeatability of the Lutetia observations.

The 1996 and 2008 spectra (Figure 1) are the only available spectra with the sub-solar point in Lutetia's southern hemisphere, with the 2008 data near polar and the 1996 data at roughly 20 S (with the sub-Earth latitude just north of the equator: Table 2 shows the observational aspects of the datasets.). The 30 September data match the 2008 spectrum within observational uncertainty at all wavelengths, although the overlap at 3.35 μm is with the 2008 uncertainty rather than the 2008 data points. Conversely, the mismatch in the 29 September data is larger than the uncertainties at 2.95 and 3.12 μm, missing the 2008 data points by 2.5-3 σ and the 2008 uncertainty by 2-2.5 σ.

It is not clear whether the differences between the 29 September and the other data are due to variations on the surface or another cause. Two objects other than Lutetia were observed on 29 September with NSFCam and subsequently with SpeX: 419 Aurelia and 10 Hygiea. Both objects have consistent spectra between those two data sets, although both also have somewhat larger error bars in the 1996 data than Lutetia (Figure 2). The CSO archive of 225 GHz τ values includes 29 and 30

September 1996, with the measurements indicating precipitable water values between 2.5 and 3.5 mm for those nights. While a direct comparison between those PW values and the measured 1996 extinction coefficients in the 3-μm region requires modeling that is beyond the scope of this paper, we note that 2.5-3.5 mm PW is well within the range of values typically handled by our reduction and analysis pipeline.

The possibility of variation on Lutetia's surface is discussed below. We use the pole position of Carry et al. (2010) for these discussions, with viewing aspect provided by use of IMCCE's Miriade VO tool[2].

4. Discussion:

4.1 Variation on Lutetia's surface?

The 29 and 30 September LXD observations were taken roughly a quarter-rotation apart, and the central longitude for the 29 September data is far from any other spectrum taken at these wavelengths, leaving the possibility that that region on Lutetia's surface is spectrally different from the rest (Table 2). The 2003/2007 north polar spectra and the 2008 south polar spectrum are roughly similar to one other, though the south pole has lower reflectance in the 3 μm spectral region and a deeper absorption band. Taken at face value, this suggests that any 3-μm absorber is more concentrated in the southern hemisphere than the northern one, but also that spectral differences in the 2-4 μm region are fairly modest.

[2] http://vo.imcce.fr/webservices/miriade/

Interestingly, however, Lazzarin et al. (2010) reported variation on the surface of Lutetia from visible and near-IR spectra, with the observed spectral range spanning the space from X-class to C-class objects, that is from red-sloped spectra to flat spectra without any absorption features. Lazzarin et al. also report the northern hemisphere of Lutetia as having a more C-like spectrum than the southern hemisphere, which has a generally more X-like spectrum or one intermediate between C and X. Nedelcu et al. (2007) also found variation on Lutetia's surface ranging from C-type to X-type near-IR spectra, with longitudinal as well as latitudinal variation. Perna et al. (2010) saw a variation in spectral slope in the visible-near IR region. Interestingly, these results are all at least qualitatively consistent with earlier observations: The 52-color spectrum of Lutetia classified Cv/M by Howell et al. (1994) is centered near the north pole, the Bus and Binzel (2002) SMASS spectrum is more equatorial but centered south of the equator and is firmly in the X complex rather than the C complex. The Rosetta OSIRIS spectrophotometric observations reported by Lamy et al. (2010) were centered within 30 degrees of the north pole and were interpreted as "completely outside [the] C" class. However, visual inspection of the OSIRIS spectrophotometric colors shows them to be at least qualitatively consistent with the Lazzarin et al. (2004) spectra obtained at similar latitudes, which Lazzarin et al. described as a "good match to the average [Bus taxonomy] C-type". A full accounting of the variation found on Lutetia, and how that variation is quantitatively mapped to Lutetia's geography, is beyond the scope of this paper. In brief summation, however, the northern hemisphere of Lutetia appears more consistent with C-class spectra, while

the southern hemisphere is more like X-class spectra, and there is evidence of eastern/western hemispheric variation in spectral slopes as well.

Most intriguingly, Lazzarin et al. reported the region of Lutetia's most C-like spectra in the southern hemisphere as occurring at a central longitude coinciding with the 29 September 1996 NSFCam observations. This is consistent with the difference between the 29 September and other 3-μm spectra being due to compositional differences. Given the LXD spectra of the northern hemisphere and its more muted (or even absent) 3-μm band, this would seem to require three distinct materials on Lutetia's surface: 1) An anhydrous material with a C-like visible-near IR spectrum for the northern hemisphere, 2) a C-like material with a relatively deeper 3-μm band for the surface feature seen by Lazzarin et al. in the southern hemisphere, and 3) an X-like material with a relatively shallower 3-μm band in other regions of the southern hemisphere. The requirement for two distinct types of C-type material is potentially problematic and does not obviously lend itself to solutions that are not in some way ad hoc. We again note, however, that the 3-μm observations considered in isolation simply imply greater absorption (and presumably hydration) in the southern hemisphere than the north. It is also clear, given the evidence in the literature, that care is required in appending and comparing spectra taken from different viewing aspects on Lutetia. Figure 3 compares 0.4-4 μm spectra for two different regions on Lutetia's surface, compiled from various sources: A southern hemisphere site centered near the 2008 LXD observations (including visible-near IR data from Perna et al. 2010 and SpeX prism-mode data reported in DeMeo et al. 2009) and a northern hemisphere site centered

near the 2007 LXD observations (including visible data from Lazzarin et al. 2004 and near-IR data from the 52-color survey of Bell et al. 1988), close to Lutetia's north pole. The full northern hemisphere spectrum is qualitatively consistent with little or no 3-μm absorption, while the southern hemisphere spectrum is consistent with a band depth of a few percent in the 3-μm region compared to a continuum extrapolated from the 2.0-2.4 μm region.

4.2 Constraints on the composition of Lutetia

The scarcity of diagnostic absorptions on Lutetia shortward of 2.5 μm has greatly hampered our understanding of its composition to this point. Vernazza (2009) proposed EL6 chondrites as a possible analog for Lutetia, fitting its spectrum to a mix of three such meteorites. However, this fit was based on overall spectral shape (including a drop in reflectance shortward of ~0.7 μm) rather than by identifying absorption bands (which, indeed, are not present in the spectra). Similarly, Nedelcu et al. identified carbonaceous chondrites and enstatite chondrites as supplying the best matches to Lutetia among the meteorites, though they did not include the albedo of Lutetia in identifying their matches. Lazzarin et al. (2009) concluded that carbonaceous chondrites were the most plausible analogs for Lutetia, with the presence of Lutetia's 3-μm band leading them to prefer metal-rich CB/CH meteorites to the anhydrous CV/CO meteorites. Several workers have identified weak absorption features near 0.43 μm, usually interpreted as evidence of a hydrated silicate (Lazzarin et al. 2004, Prokof'eva et al. 2005, Busarev et al. 2010)

though Lazzarin et al. (2009) noted the absorptions appear in some non-hydrated minerals as well.

Looking longward of 2.5 μm, the NSFCam spectrophotometry is of low spectral resolution, leaving the SpeX data as the best dataset for compositional analysis (though of course any such analysis must be consistent with the other datasets). We can note that Lutetia's 3-μm spectrum is unlike those seen in low albedo asteroids. Though no formal taxonomy of 3-μm asteroid data has been undertaken, Rivkin (2010, also Rivkin et al. in preparation) qualitatively described 3-4 different band shapes, named after their most prominent members: Ceres-type, Pallas-type, and Themis-type, as well as "no band". These types are shown in Figure 4. Lutetia, as can be seen, does not have the linear (or "checkmark") shape seen in 2 Pallas or CM chondrites, neither does it obviously appear to have a band shape attributable to ice frost like that of 24 Themis (Rivkin and Emery 2010, Campins et al. 2010) or like the one on 1 Ceres that Milliken and Rivkin (2009) attributed to brucite. It is also a different band shape than has been reported for water/OH on the lunar surface (Pieters et al. 2009, Sunshine et al. 2009, Clark 2009). As a result, we do not think the types of hydrated minerals found on these other objects (serpentine, tochilinite, brucite) are present on Lutetia's surface. There is some evidence that 3-μm band shapes similar to Lutetia's may be found in other X-complex asteroids, but additional analyses on those asteroids are still underway (Rivkin et al., in preparation).

Beck et al. (2010) suggested goethite (FeO(OH)) as a possible mineral on low-albedo asteroid surfaces as an explanation for their 3-μm band shapes, and

Fornasier et al (2010) included goethite as a component in their best-fit mixing models for M asteroids in the 0.5-2.5 μm region. Goethite has a broad, shallow 3-μm band, with a minimum near 3.1-3.2 μm. Figure 5 shows goethite can qualitatively match the 2008 LXD spectrum when in a linear mixture of 7% goethite 93% neutral material. A higher amount of goethite (20%) will match the lower-resolution 29 September 1996 NSFCam spectrum. We note that this simple type of mixture does not necessarily reflect the actual fraction of goethite present on Lutetia's surface, though it does qualitatively demonstrate the plausibility of its presence there.

We can increase the wavelength range under consideration by adding a prism-mode (0.8-2.5 μm) spectrum from the DeMeo et al. (2009) and a visible-wavelength spectrum from Perna et al. (2010). These shorter-wavelength data have fairly close matches to the 2008 LXD viewing aspect, as discussed above. The goethite plus neutral material mixture is less adequate in the visible region: it is within ~2-3% of Lutetia's spectrum but contains absorptions not obviously seen on Lutetia, most notably absorptions at ~0.9 μm and ~0.65 μm. This mismatch is the most obvious drawback to the interpretation of goethite, and either provides a constraint on the maximum concentration of goethite or else requires a somewhat ad hoc and hypothetical requirement on particle size. In addition, the 0.9-μm band depth in the 20% goethite mix, which matched the 29 September 1996 NSFCam data, is deeper than can be accommodated by the existing visible-NIR spectra of Lutetia taken at a similar sub-Earth/sub-solar location (Nedelcu et al. 2007)

If iron is available in its surface minerals (whether in silicates, goethite, or other oxides: Zhang and Keller 2010, for instance), we might expect the creation and

deposition of nanophase iron (npFe) via space weathering, as is seen in mature lunar samples and whose presence is inferred in asteroidal regolith. In order to investigate the possible effects of space weathering on a goethite composition, we used spreadsheets created by and described in Quinn et al. (2010) to generate optical constants for goethite. The goethite spectrum was obtained from the RELAB website[3], with Hiroi as PI. The goethite optical constants were then used to model the spectral effects of a npFe coating following the work of Hapke (2001) and Shkuratov et al. (1999), allowing us to forward model differing grain sizes and amounts of npFe. While the model results are non-unique, they do serve as a plausibility check and a means of testing possible compositions. In addition to the linear model discussed above, figure 5 also includes the model spectrum of space weathered goethite compared to the southern hemisphere combined spectrum of Lutetia.

Goethite is not a common mineral in meteorites, though it can be created through weathering of ordinary chondrite material (Lee et al. 2006). It is conceivable that goethite could have formed via very small amounts of aqueous alteration of an iron metal-rich surface, with only small amounts of water available. However, given the information currently available it is difficult to treat this as more than speculation. Similarly, it is difficult to make useful predictions of whether the north-south difference in band depth is due to a (presumed) goethite-bearing layer being exposed in the south after impact excavation or due to such a layer being buried or dehydrated in the north. The anticipated geological interpretations and

[3] http://www.planetary.brown.edu/relabdata/

cratering history of Lutetia as derived from Rosetta data should help constrain these speculations.

Troilite (FeS) has been proposed as a possible cause of 3-μm features on W asteroids (Cloutis and Burbine 1999) though Rivkin et al. (2002) discussed several critical problems with the idea. The Pollack et al. (1994) optical constants for troilite do not lead to any absorption centered near 3 μm, in line with the expectations of Rivkin et al. Troilite may be present on Lutetia's surface, but it does not appear to be the cause of any 3-μm band.

The northern hemisphere spectrum is rather free of absorption bands, and is strikingly flat longward of ~0.6 μm. The lack of strong absorptions in the 3-μm region does not place any new constraints on previous work, and neither does it provide any opportunity for diagnostic identification of minerals. Vernazza et al. (2009) did not publish their spectral fits to Lutetia beyond 2.5 μm, and given the difficulty of removing terrestrial water from anhydrous samples, it is possible the fits to that wavelength region would be of limited use in any event. The Vernazza et al. interpretation of Lutetia's spectrum (technically of its northern hemisphere data) as consistent with a mixture of enstatite chondrites is thus also consistent with our data. It is perhaps worth noting, however, the apparent ineffectiveness of space weathering on the spectrum of Lutetia's northern hemisphere: Vernazza et al found that irradiation experiments on the enstatite chondrite Eagle (EL6) did not produce significant changes in its spectrum, and performed fits using unaltered material.

The lack of a significant 3-μm band in Lutetia's northern hemisphere, in addition to putting limits on the amount of hydrated minerals, also suggests that OH/H_2O has

not been created by solar wind interactions with silicates in Lutetia's regolith since the north-south variation is not consistent with an external cause like the solar wind. This stands as a contrast to the interpretations of the 3-μm absorption seen in the lunar regolith (Pieters et al. 2009, Sunshine et al. 2009, Clark 2009) and the hypothesized formation of the OH/H_2O responsible.

4.3 Expectations for Rosetta/Future Work

Lutetia's northern hemisphere was visible during the Rosetta encounter (Carry et al. 2010) and unfortunately the regions with the deepest 3-μm bands are likely to be in shadow, beyond the limb, or at the very least in very unfavorable geometries for observation. It seems likely that Rosetta-derived spectra of Lutetia will be like the northern hemisphere compilation presented here, and like the spectra fit by Vernazza et al.

Lutetia begins northern autumn in October 2011 and the sub-Earth and sub solar points are in Lutetia's southern hemisphere from then until September 2013. While it will be fainter than its 2011 apparition, it will still be a relatively easy telescopic target compared to many asteroids of interest. There is intriguing evidence from multiple authors using various instruments throughout the 0.4-4 μm region that Lutetia shows some spectral variation, which is a rarity among asteroids.

4.3 Is there a good meteorite analog to Lutetia?

The majority of publications concerned with Lutetia's composition liken it to either enstatite chondrites or carbonaceous chondrites. The spectral datasets

available at this writing point in different directions depending upon the wavelength region and whether the focus is on spectral slopes or absorptions. Non-spectral datasets, like radar and polarimetry, also provide ambiguous results.

The existence of mixed-class meteorites like Kaidun and Almahatta Sitta could be used to argue that Lutetia could be a similar mixture of unlike meteorite types, in this case enstatite chondrite and carbonaceous chondrite. However, it is not obvious how to both bring those materials together but keep them mostly-segregated on a regional-to-hemispheric scale, as the spectral data would require. Nor, if forced to choose between carbonaceous or enstatite chondrite, is it obvious which meteorite type is the most apt analog for Lutetia. The CH and CB chondrites have some of the general properties one might expect of a Lutetia-like meteorite, but the only published spectra for CB/CH meteorites do not have 3-μm band centers like those seen on Lutetia (Osawa et al. 2005).

However, we should not consider ourselves forced to choose only between the enstatite and carbonaceous chondrites. Lutetia is not associated with any dynamical families, and it is not particularly close to any resonances. As a result, and with no mitigating circumstances, Lutetia need not be considered a particularly significant contributor to the NEO population or the meteorite collection (Morbidelli et al. 1994, Bottke, pers. comm.). Given the still-ambiguous nature of the data in hand and the imperfect matches to what we expect, the best choice for Lutetia's meteorite analog may be "none of the above".

5. Conclusions:

Observations of 21 Lutetia in the 3-μm region are compiled and analyzed. An absorption of variable depth is seen, consistent with a greater amount of hydrated minerals in the southern hemisphere, with less in the northern hemisphere. These variations are consistent with variations seen by other workers in other wavelength regions, suggesting in the simplest case a material with a flatter spectral slope and shallow or no 3-μm absorption dominating the northern hemisphere, a material with more appreciable spectral slope and a ~3-5% absorption over part of the southern hemisphere (depending on choice of continuum level), and a third material with deeper 3-μm absorption but a flatter visible-near IR spectrum in one particular area in the southern hemisphere. The distribution of surface materials presented here may be only one of many possible explanations for the diverse datasets available.

The scarcity of spectral features shortward of 2.5 μm makes diagnostic compositional work difficult to undertake, but the southern hemisphere absorption in the 3-μm region is at least qualitatively consistent with a contribution from a few percent of goethite. While some interpretations favor carbonaceous chondrites as analogs for Lutetia and others enstatite chondrites, we note that Lutetia may not have any good analogs among the meteorites.

Acknowledgments:

This research has made use of IMCCE's Miriade VO tool. Our thanks to Benoit Carry, who provided much useful information and enabled us to determine Lutetia's

aspect at the times of our (and other) observations. Our observations were funded by grant NNG05GR60G from the NASA Planetary Astronomy Program, and reduction and analysis by grant NNX1AG40G from the NASA Planetary Geology and Geosciences Program. Continued thanks to the people of Hawaii for allowing us to use Mauna Kea for observations, and continued thanks to the stalwart telescope operators of the NASA IRTF. Merci beaucoup to Richard Binzel. Some of the data utilized in this publication were obtained and made available by the the MIT-UH-IRTF Joint Campaign for NEO Reconnaissance. The MIT component of this work is supported by the National Science Foundation under Grant No. 0506716.

References

Barucci, M. A., Fornasier, S., Dotto, E., Lamy, P. L., Jorda, L., Groussin, O., Brucato, J. R., Carvano, J., Alvarez-Candal, A., Cruikshank, D., and Fulchignoni, M. (2008). Asteroids 2867 Steins and 21 Lutetia: surface composition from far infrared observations with the Spitzer space telescope. *Astron. Astroph*, 477:665–670.

Barucci, M. A., Fulchignoni, M., Fornasier, S., Dotto, E., Vernazza, P., Birlan, M., Binzel, R. P., Carvano, J., Merlin, F., Barbieri, C., and Belskaya, I. (2005). Asteroid target selection for the new Rosetta mission baseline. 21 Lutetia and 2867 Steins. *Astron. Astroph*, 430:313–317.

Beck, P., Quirico, E., Sevestre, D., Montes-Hernandez, G., Pommerol, A., and Schmitt, B. (2011). Goethite as an alternative origin of the 3.1 μm band on dark asteroids. *Astron. Astroph*, 526:A85-89.

Bell, J. F., Owensby, P. D., Hawke, B. R., and Gaffey, M. J. (1988). The 52-color asteroid survey: Final results and interpretation. *LPSC XIX*:57.

Birlan, M., Vernazza, P., Fulchignoni, M., Barucci, M. A., Descamps, P., Binzel, R. P., and Bus, S. J. (2006). Near infra-red spectroscopy of the asteroid 21 Lutetia. I. New results of long-term campaign. *Astron. Astroph.*, 454:677–681.

Bus, S. J. and Binzel, R. P. (2002). Phase II of the Small Main-Belt Asteroid Spectroscopic Survey: A Feature-Based Taxonomy. *Icarus*, 158:146–177.

Busarev, V. V. (2010). Spectral Studies of Asteroids 21 Lutetia and 4 Vesta as Objects of Space Missions. *Solar Syst. Res.* 44:507-519.

Campins, H., Hargrove, K., Pinilla-Alonso, N., Howell, E. S., Kelley, M. S., Licandro, J., Mothé-Diniz, T., Fernández, Y., and Ziffer, J. (2010). Water ice and organics on the surface of the asteroid 24 Themis. *Nature*, 464:1320–1321.

Carry, B., Kaasalainen, M., Leyrat, C., Merline, W. J., Drummond, J. D., Conrad, A., Weaver, H. A., Tamblyn, P. M., Chapman, C. R., Dumas, C., Colas, F., Christou, J. C., Dotto, E., Perna, D., Fornasier, S., Bernasconi, L., Behrend, R., Vachier, F., Kryszczynska, A., Polinska, M., Fulchignoni, M., Roy, R., Naves, R., Poncy, R., and Wiggins, P. (2010). Physical properties of the ESA Rosetta

target asteroid (21) Lutetia. II. Shape and flyby geometry. *Astron. Astroph.*, 523:A94-110.

Clark, B. E., Ziffer, J., Nesvorny, D., Campins, H., Rivkin, A. S., Hiroi, T., Barucci, M. A., Fulchignoni, M., Binzel, R. P., Fornasier, S., DeMeo, F., Ockert-Bell, M. E., Licandro, J., and Mothé-Diniz, T. (2010). Spectroscopy of B-type asteroids: Subgroups and meteorite analogs. *Journal of Geophysical Research (Planets)*, 115:6005–6026.

Clark, R. N. (2009). Detection of Adsorbed Water and Hydroxyl on the Moon. *Science*, 326:562–.

Cloutis, E. A. and Burbine, T. H. (1999). The spectral properties of troilite/pyrrhotite and implications for the E-asteroids. *LPSC* XXX. abst. no. 18.75.

Cushing, M. C., Vacca, W. D., and Rayner, J. T. (2003). Spextool: A Spectral Extraction Package for SpeX, a 0.8-5.5 micron Cross-Dispersed Spectrograph. *PASP*, 115:383–388.

Delbó, M., Dell'Oro, A., Harris, A. W., Mottola, S., Mueller, M. (2007). Thermal inertia of near-Earth asteroids and implications for the magnitude of the Yarkovsky effect. *Icarus*, 190:236-249.

Delbó, M., Harris, A. W., Binzel, R. P., Pravec, P., and Davies, J. K. (2003). Keck observations of near-Earth asteroids in the thermal infrared. *Icarus*, 166:116–130.

DeMeo, F. E., Binzel, R. P., Slivan, S. M., and Bus, S. J. (2009). An extension of the Bus asteroid taxonomy into the near-infrared. *Icarus*, 202:160–180.

Howell, E. S., Merényi, E., and Lebofsky, L. A. (1994). Classification of asteroid spectra using a neural network. *Journal of Geophysical Research (Planets*) 99:10847–10865.

Lamy, P. L., Faury, G., Jorda, L., Kaasalainen, M., and Hviid, S. F. (2010). Multi-color, rotationally resolved photometry of asteroid 21 Lutetia from OSIRIS/Rosetta observations. *Astron. Astroph.*, 521:A19-28.

Lazzarin, M., Marchi, S., Magrin, S., and Barbieri, C. (2004) Visible Spectral Properties of Asteroid 21 Lutetia, Target of Rosetta Mission, *Astron. Astrophys.* 425:L25–L28

Lazzarin, M., Marchi, S., Moroz, L. V., & Magrin, S. (2009) New visible spectra and mineralogical assessment of (21) Lutetia, a target of the Rosetta mission. *Astron. Astroph.*, 498:307-311

Lazzarin, M., Magrin, S., Marchi, S., Dotto, E., Perna, D., Barbieri, C., Barucci, M. A., and Fulchignoni, M. (2010). Rotational variation of the spectral slope of (21) Lutetia, the second asteroid target of ESA Rosetta mission. *Mon. Not. R. astr. Soc*, 408:1433–1437.

Lebofsky, L. A., Sykes, M. V., Tedesco, E. F., Veeder, G. J., Matson, D. L., Brown, R. H., Gradie, J. C., Feierberg, M. A., and Rudy, R. J. (1986). A refined "standard" thermal model for asteroids based on observations of 1 Ceres and 2 Pallas. *Icarus*, 68:239–251.

Lupishko, D. F. and Belskaya, I. N. (1989). On the surface composition of the M-type asteroids. *Icarus*, 78:395–401.

Magri, C., Ostro, S. J., Rosema, K. D., Thomas, M. L., MItchell, D. L., Campbell, D. B., Chandler, J. F., Shapiro, I., Giorgini, J. D., and Yeomans, D. K. (1999). Mainbelt asteroids: Results of Arecibo and Goldstone radar observations of 37 objects during 1980-1995. *Icarus*, 140:379-407.

Milliken, R. E., and Rivkin, A. S. (2009). Brucite and carbonate assemblages from altered olivine-rich materials on Ceres. *Nature Geo*. 2:258-261.

Morbidelli, A., Gonczi, R., Froeschle, C., and Farinella, P. (1994). Delivery of meteorites through the ν6 secular resonance. *Astron. Astroph.*, 282:955–979.

Nedelcu, D. A., Birlan, M., Vernazza, P., Descamps, P., Binzel, R. P., Colas, F., Kryszczynska, A., and Bus, S. J. (2007). Near infra-red spectroscopy of the asteroid 21 Lutetia. II. Rotationally resolved spectroscopy of the surface. *Astron. Astroph.*, 470:1157–1164.

Osawa, T., Kagi, H., Nakamura, T., and Noguchi, T. (2005). Infrared spectroscopic taxonomy for carbonaceous chondrites from speciation of hydrous components. *Met. Plan. Sci*. 40:71-86.

Perna, D., Dotto, E., Lazzarin, M., Magrin, S., Fulchignoni, M., Barucci, M. A., Fornasier, S., Marchi, S., and Barbieri, C. (2010). Inhomogeneities on the surface of 21 Lutetia, the asteroid target of the Rosetta mission. Ground-based results before the Rosetta fly-by. *Astron. Astroph.*, 513:L4-6.

Pieters, C. M., Goswami, J. N., Clark, R. N., Annadurai, M., Boardman, J., Buratti, B., Combe, J., Dyar, M. D., Green, R., Head, J. W., Hibbitts, C., Hicks, M., Isaacson, P., Klima, R., Kramer, G., Kumar, S., Livo, E., Lundeen, S., Malaret, E., McCord, T., Mustard, J., Nettles, J., Petro, N., Runyon, C., Staid, M., Sunshine, J., Taylor, L. A., Tompkins, S., and Varanasi, P. (2009). Character and Spatial Distribution of OH/H_2O on the Surface of the Moon Seen by M on Chandrayaan-1. *Science*, 326:568

Pollack, J. B., Hollenbach, D., Beckwith, S., Simonelli, D. P., Roush, T., and Fong, W. (1994). Composition and radiative properties of grains in molecular clouds and accretion disks. *Ap. J.*, 421:615–639.

Prokof'eva, V.V., Bochkov, V.V., and Busarev, V.V., (2005) The Surface Structure of the M–Type Asteroid 21 Lutetia: Spectral and Frequency Analysis, *Solar Syst. Res.* 39:410-420.

Quinn, D. P., Gillis-Davis, J. J., and Lucey, P. G. (2010). Using Microsoft Excel for Hapke Modeling: A Technique to Simplify Calculations of Optical Constants and Reflectance Spectra. *LPSC* 41:abst. #2426.

Rivkin, A. S. (2010) The Diversity of Hydrated Material on Low-Albedo Asteroids. *Bull. Amer. Ast. Soc.* 42: abstract #53.08.

Rivkin, A. S. and Emery, J. P. (2010). Detection of ice and organics on an asteroidal surface. *Nature*, 464:1322–1323.

Rivkin, A. S., Howell, E. S., Vilas, F., and Lebofsky, L. A. (2002). Hydrated minerals on asteroids: The astronomical record. In Bottke, W., Cellino, A., Paolicchi, P., and Binzel, R. P., editors, *Asteroids III*, pages 235–253. University of Arizona Press, Tucson.

Rivkin, A. S., Lebofsky, L. A., Clark, B. E., Howell, E. S., and Britt, D. T. (2000). The nature of M-class asteroids in the 3-μm region. *Icarus*, 145:351–368.

Rivkin, A. S., McFadden, L. A., Binzel, R. P., and Sykes, M. (2006). Rotationally-resolved spectroscopy of Vesta I: 2 4 μm region. *Icarus*, 180:464–472.

Shepard, M. K., Clark, B. E., Ockert-Bell, M., Nolan, M. C., Howell, E. S., Magri, C., Giorgini, J. D., Benner, L. A. M., Ostro, S. J., Harris, A. W., Warner, B. D., Stephens, R. D., Mueller, M. (2010). A radar survey of M- and X-class asteroids II. Summary and synthesis. *Icarus*, 208:221-237.

Shkuratov, Y., Starukhina, L., Hoffmann, H., and Arnold, G. (1999). A Model of Spectral Albedo of Particulate Surfaces: Implications for Optical Properties of the Moon. *Icarus*, 137:235–246.

Sunshine, J. M., Farnham, T. L., Feaga, L. M., Groussin, O., Merlin, F., Milliken, R. E., and A'Hearn, M. F. (2009). Temporal and Spatial Variability of Lunar Hydration As Observed by the Deep Impact Spacecraft. *Science*, 326:565–568.

Tedesco, E. F., Veeder, G. J., Fowler, J. W., and Chillemi, J. R. (1992). *The IRAS Minor Planet Survey Data Base*. National Space Science Data Center, Greenbelt, Maryland. digital data.

Tholen, D. J. (1984). *Asteroid taxonomy from cluster analysis of photometry*. Ph.D. dissertation, University of Arizona, Tucson, AZ.

Vernazza, P., Brunetto, R., Binzel, R. P., Perron, C., Fulvio, D., Strazzulla, G., and Fulchignoni, M. (2009). Plausible parent bodies for enstatite chondrites and mesosiderites: Implications for Lutetia's fly-by. *Icarus*, 202:477–486.

Volquardsen, E. L., Rivkin, A. S., and Bus, S. J. (2007). Composition of hydrated near-Earth object (100085) 1992 UY4. *Icarus*, 187:464–468.

Yang, B. and Jewitt, D. (2010). Identification of Magnetite in B-type Asteroids. *Astron. J.*, 140:692–698.

Zhang, S. and Keller, L. P. (2010). Probing the Iron Oxidation State of Space-Weathered Rims on Lunar Soil Grains at Nm-Scale. *Meteoritics and Planetary Science Supplement*, 73:abst. #5383.

Tables

Date (UT)	V Mag	Phase Angle	Solar Dist (AU)	Earth Dist (AU)	Standards	Integration time (s)
2 Mar 2003	12.1	20.7°	2.60	2.06	L102-1081, SAO 65083	720
31 Mar 2007	11.7	21.9°	2.42	1.84	HD 140990, HD 153631	1800
23 Dec 2008	10.5	10.9°	2.46	1.55	HD 12846, Hya 64	1260

Table 1: Observing Circumstances for SpeX data

UT Time	SE Lon	SE Lat	SS Lon	SS Lat	Note	2.95 μm/ 2.4 μm	3.12 μm/2.3 μm
9/29/96 9:30	227	+3.3	223	-17.8	NSFCam	0.88 ± 0.03	0.87 ± 0.03
9/30/96 8:00	316	+3.3	312	-18.1	NSFCam	0.95 ± 0.04	0.90 ± 0.06
3/2/03 14:18	124	+85.5	161	+65.9	Spex LXD	1.00 ± 0.02	0.97 ± 0.02
3/31/07 14:57	358	+67.3	72	+85.2	Spex LXD	1.02 ± 0.02	0.98 ± 0.02
12/23/08 9:26	120	-77.6	108	-67.3	Spex LXD	0.95 ± 0.02	0.94 ± 0.02
7/10/10	---	---	---	+46.6	Rosetta	---	---

Table 2: Sub-Earth (SE) and sub-solar (SS) coordinates at times of observation for NSFCam and Spex data, and for Rosetta flyby. The latitudes and longitudes presented here were obtained via IMCCE's Miriade VO tool, using the rotational pole coordinates of Carry et al. (2010).

Figures

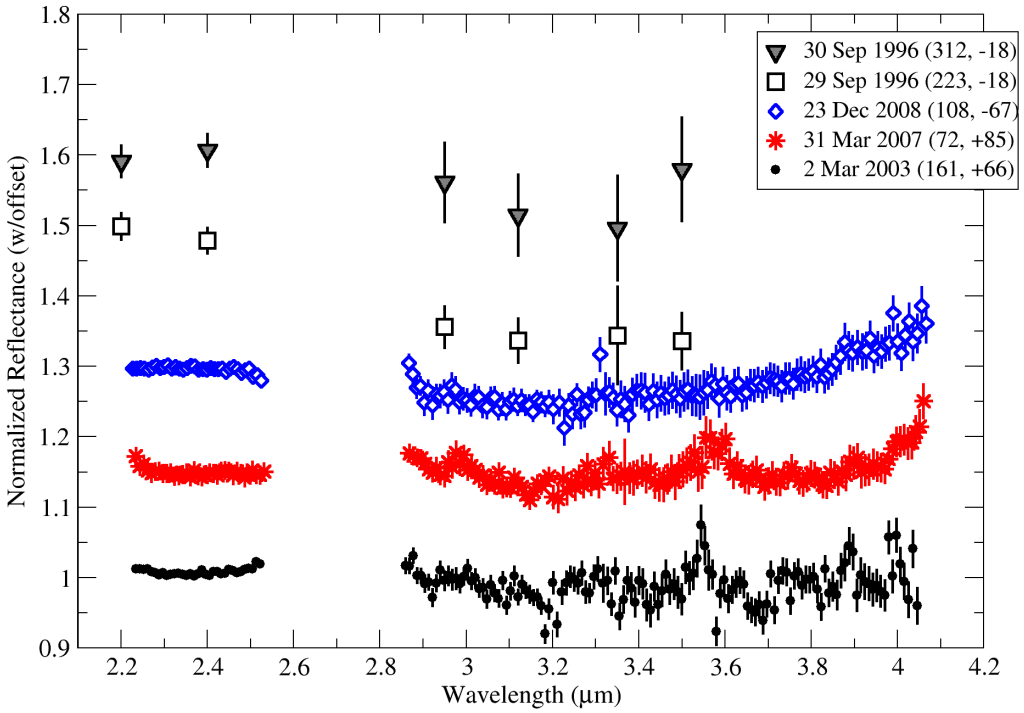

Figure 1: 2-4 μm spectra for Lutetia, from NSFCam and SpeX. Spectra are normalized to 2.3 μm and offset for clarity. The gap between ~2.5-2.8 μm is due to the Earth's atmosphere, where transmission is low enough to hamper data collection. The sub-solar latitude and longitude for each observation is also included in the legend.

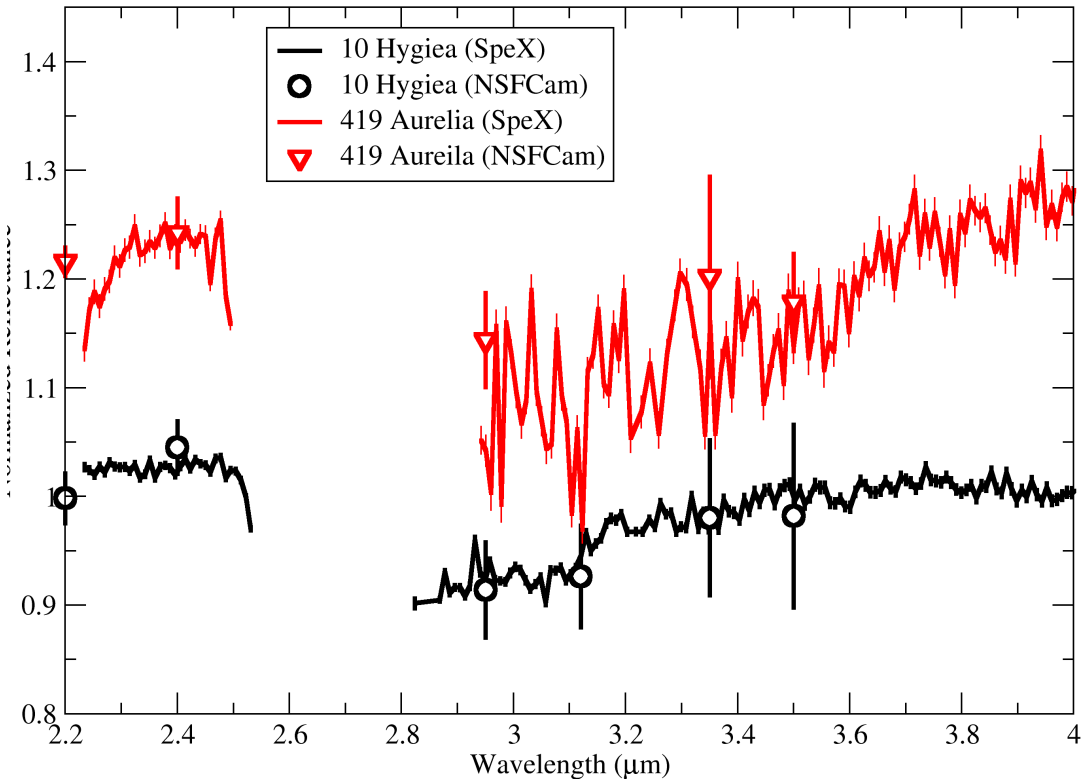

Figure 2: NSFCam observations from 29 September 1996 (open symbols) compare favorably to later SpeX observations (lines). While these datasets, offset for clarity, are of lower S/N than the Lutetia observations, the agreement between them suggests the discrepancies between the 29 September 1996 Lutetia observations and later SpeX observations are due to real differences and not observational factors.

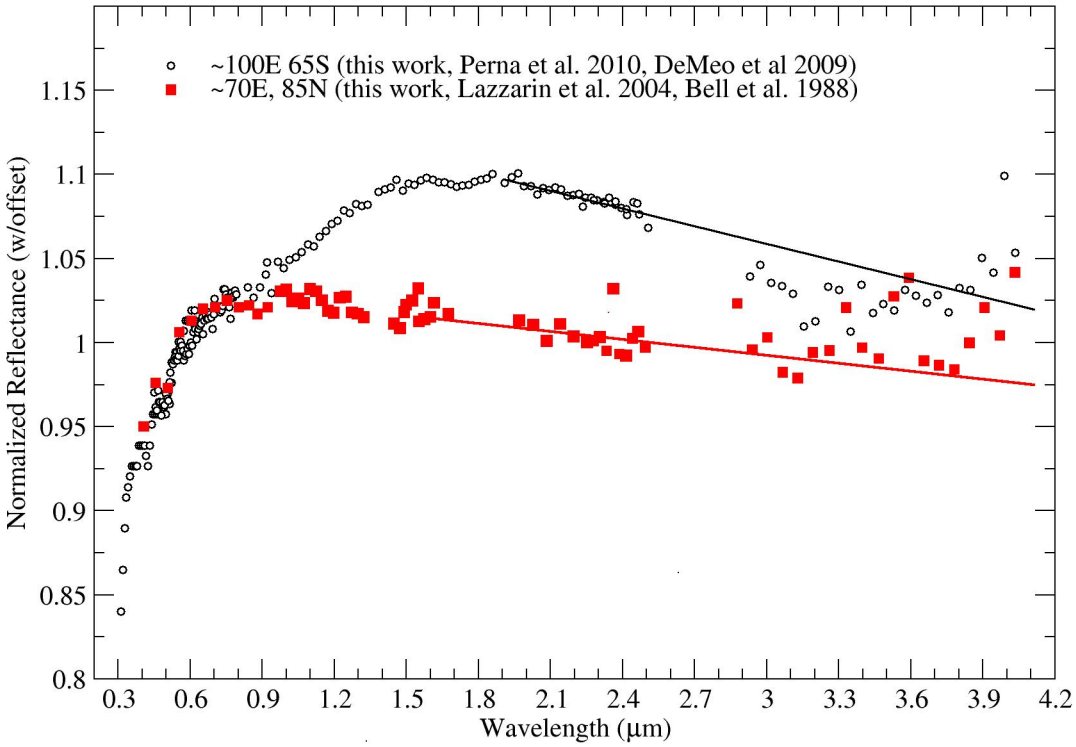

Figure 3: Compilations of 0.3-4 μm spectra of Lutetia from various sources shows large differences between the northern (closed, red symbols) and southern (open black symbols) hemispheres. Furthermore, the southern hemisphere shows absorption in the 3-μm region compared to an extrapolated continuum (solid line) while the northern hemisphere shows no obvious absorption.

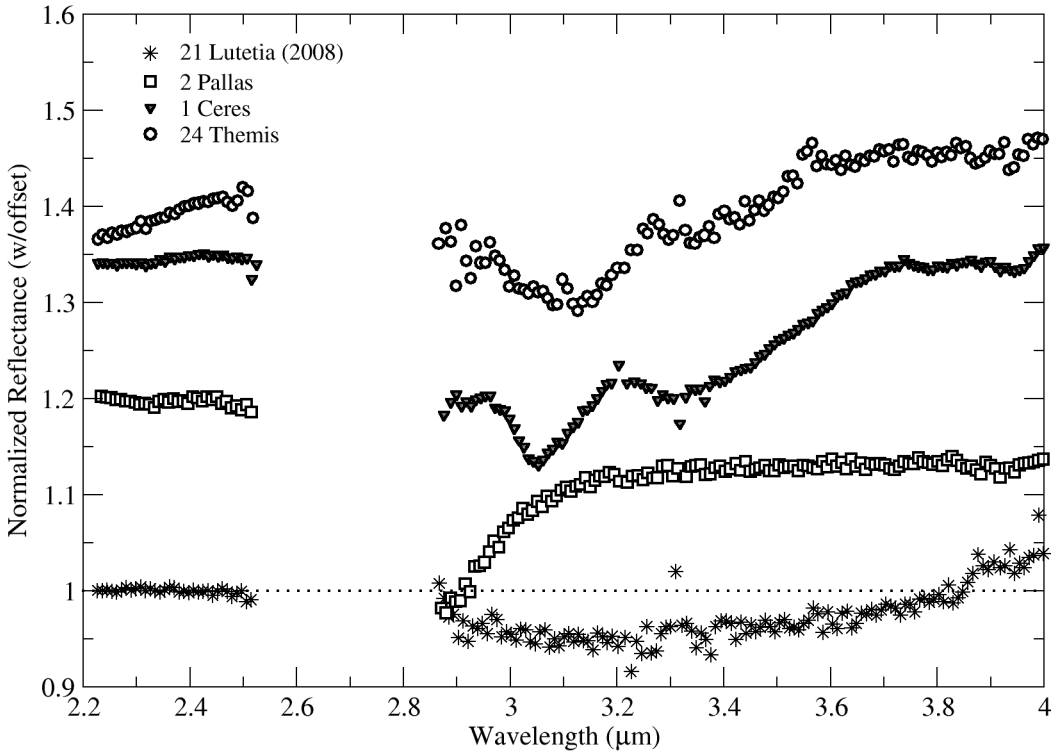

Figure 4: Lutetia's absorption in the 3-μm region does not resemble that of other hydrated objects, shown above. Ceres, Pallas, and Themis represent the three most common band shapes among C-complex objects, interpreted as due to brucite and carbonates, CM-like phyllosilicates, and ice frost respectively. A dotted line is also included to demonstrate Lutetia's band shape relative to a flat continuum.

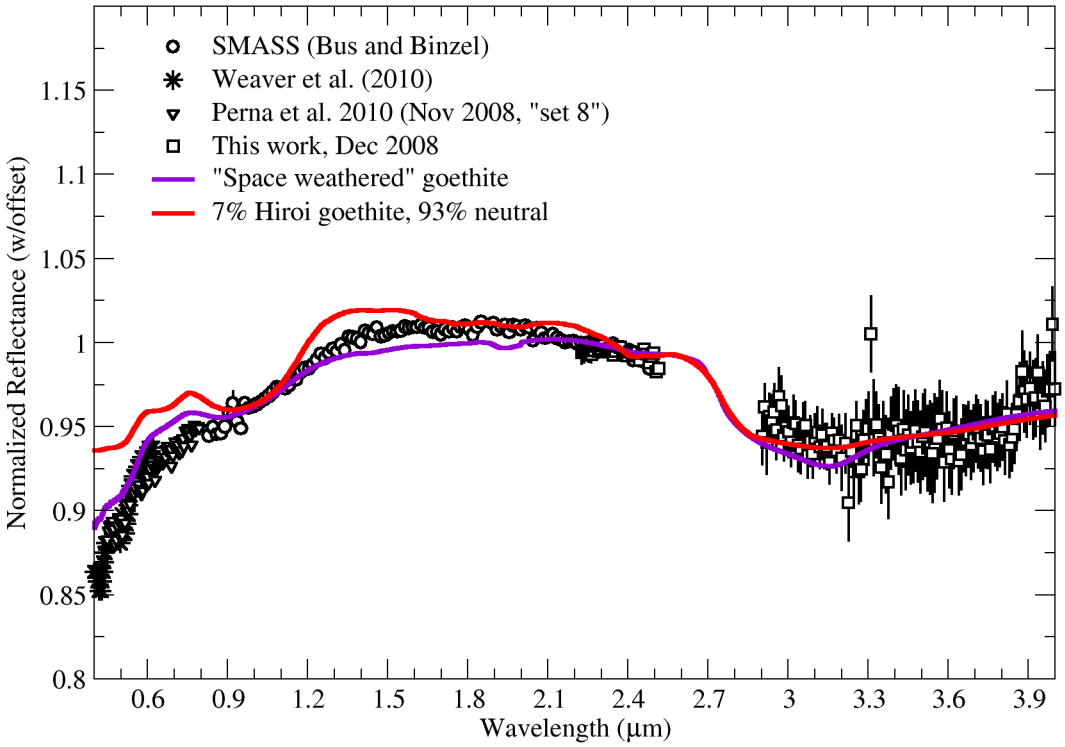

Figure 4: The 2-4 μm spectrum of Lutetia (symbols) can be qualitatively matched with a mixture (red) of 7% goethite and 93% neutral material (to decrease the band depth). However, the match is poorer outside this wavelength region. The full 0.4-4μm spectrum of regions on Lutetia's southern hemisphere can be qualitatively matched by space weathered goethite (violet). More detailed models will be necessary to determine to what extent this is consistent with spectra of other regions on Lutetia, particular the northern hemisphere areas observed by Rosetta.